Front. Earth Sci. 2023, 17(3): 760−775
https://doi.org/10.1007/s11707-022-1025-y

RESEARCH ARTICLE

Effects of sub-/super-critical CO_2 on the fracture-related mechanical characteristics of bituminous coal

Zedong SUN[1,3], Hongqiang XIE (✉)[2], Gan FENG[2], Xuanmin SONG[1], Mingbo CHI[4], Tao MENG[5], Bole SUN[6]

1 Key Laboratory of *In-situ* Property Improving Mining (Ministry of Education), Taiyuan University of Technology, Taiyuan 030024, China
2 State Key Laboratory of Hydraulics and Mountain River Engineering, College of Water Resource & Hydropower, Sichuan University, Chengdu 610065, China
3 College of Coal Engineering, Shanxi Datong University, Datong 037003, China
4 State Key Laboratory of Water Resource Protection and Utilization in Coal Mining, Beijing 102200, China
5 School of Chemical and Biological Engineering, Taiyuan University of Science and Technology, Taiyuan 030024, China
6 China Railway Third Bureau Group Co., Ltd., Taiyuan 030001, China

Abstract Injecting carbon dioxide CO_2 into a coal seam is an important way to improve coalbed methane recovery and to store geological carbon. The fracture mechanical characteristics of bituminous coal determine the propagation and evolution of cracks, which directly affect CO_2 storage in coal seams and the efficiency of resource recovery. This study applied CO_2 adsorption and three-point bending fracture experiments using bituminous coal samples in a gaseous state (4 MPa), subcritical state (6 MPa), and supercritical state (8 and 12 MPa) to investigate the influence of CO_2 state and anisotropy on the fracture-related mechanical response of bituminous coal. The results show that the change in mechanical properties caused by CO_2 adsorption is CO_2 state-dependent. The supercritical CO_2 adsorption at 8 MPa causes the largest decrease in the mode-I fracture toughness (K_{IC}), which is 63.6% lower than the toughness before CO_2 adsorption. The instability characteristics of bituminous coal show the transformation trend of "sudden-gradual-sudden fracture". With or without CO_2 adsorption, the order of the K_{IC} associated with three types of bituminous coal specimens is crack-divider type > crack-arrester type > crack-short transverse type. Phenomenologically, the fracture toughness of bituminous coal is positively correlated with its specific surface area and total pore volume; the toughness is negatively correlated with its average pore size.

Keywords energy development, CO_2 geological storage, rock mechanics, bituminous coal

Received September 2, 2022; accepted October 10, 2022

E-mail: alex_xhq@scu.edu.cn

1 Introduction

As human society rapidly develops, an increasing amount of energy is needed (Liu and Nie, 2016; Gao et al., 2021; Liu et al., 2021a; Liu et al., 2022a; Liu et al., 2022b; Souley Agbodjan et al., 2022; Zhao et al., 2022). Fossil energy combustion creates significant greenhouse gas emissions, causing environmental pollution (Lampert, 2019). It is generally believed that the geological storage of carbon dioxide (CO_2) is an effective way to realize carbon neutralization (Say and Yücel, 2006; Raza et al., 2019). The geological storage of CO_2 in coal seams has great potential, and has attracted attention around the world (Niu et al., 2020; Mabuza et al., 2022). Due to the strong adsorption capacity of coal, carbon dioxide is easily adsorbed and sealed in coal seams, providing long-term stable storage (Qiu et al., 2020; Czerw et al., 2021). CO_2 is adsorbed in coal better than CH_4 (Liu et al., 2019c; Omotilewa et al., 2021), and CO_2 also has a good displacement effect on coalbed methane. Therefore, carbon emissions can be reduced and Coal Bed Methane (CBM) resources can be exploited simultaneously by storing carbon dioxide storage in coal seams. A coal seam that has been disturbed by geological deposition and mining has a complex fracture network structure. When CO_2 is injected and adsorbed, *in situ* stress and disturbance stress act together. Once the stress at the crack tip reaches the fracture pressure of the reservoir, cracking and instability occur, directly affecting CO_2 storage. Therefore, to better understand how a coal seam responds mechanically to CO_2, it is important to study the influence of CO_2 on the fracture characteristics of a coal seam.

It is estimated that when the buried depth of the target coal seam for the geological storage of CO_2 is ⩾ 800 m, the temperature and pressure of the reservoir exceed the supercritical point of carbon dioxide (temperature ⩾ 31.1°C, pressure ⩾ 7.38 MPa) (Patel et al., 2016). Supercritical CO_2 (S_CCO_2) has a high diffusion coefficient, low viscosity, and liquid-like density (Feng et al., 2019). This makes it easy for S_CCO_2 molecules to penetrate and diffuse into the micro pores in the coal matrix, and physically and chemically react with the coal matrix (Yin et al., 2016). In minerals rich in organic matter, such as shale or coal, CO_2 can displace a certain amount of CH_4 (Liu et al., 2017; Liu et al., 2019a; Cheng et al., 2021). After carbon dioxide is injected into the coal seam, some organic groups and mineral components in the coal are extracted. This may trigger the shrinkage and expansion of the coal matrix (Farmer and Pooley, 1967; Liu et al., 2019b; Liu et al., 2021b). The change in the coal microstructure also leads to the plasticization and softening effect of coal (Liao et al., 2021; Niu et al., 2021; Liu et al., 2022d).

The phase state of CO_2 and the saturation time significantly impact the mechanical strength of coal (Hedges et al., 2007; Ranjith and Perera, 2012; Perera et al., 2013; Ranathunga et al., 2016; Zagorščak and Thomas, 2018; Zhang et al., 2021a). This deterioration becomes increasingly significant as the CO_2 saturation pressure increases. Perera et al. (2013) and Ranathunga et al. (2016) reported that, with the increase in adsorption time of supercritical CO_2 on lignite, the uniaxial compressive strength (UCS) and elastic modulus (E) decrease by 46% and 22.71%, respectively. This is because supercritical CO_2 has a high adsorption potential, changing lignite from brittle to plastic state, and expanding the coal matrix. When CO_2 changes from a subcritical state to a supercritical state, the mechanical properties rapidly deteriorate (Zagorščak and Thomas, 2018). Clearly, CO_2 adsorption impacts the physical and mechanical properties of coal. However, the degree of this influence and the laws governing it are also related to the layered structure of coal. The bedding of coal has an effect on its mechanical properties (Tan et al., 2018; Feng et al., 2020c; Gao et al., 2020; Guo et al., 2021a; Keboletse et al., 2021; Ma et al., 2021; Nikolenko et al., 2021). Under uniaxial compression, as the loading direction and bedding angle increase, the variation of compressive strength of rock follows a U-shape (Chen et al., 2014; Hou et al., 2020). The laws governing the variations in rock when exposed to Brazilian disc splitting are similar to the laws during uniaxial compression (Liu et al., 2013; Zhao et al., 2017).

Past studies have found that the physical and mechanical properties of coal are affected to different degrees after interacting with supercritical CO_2. In fact, during the process of injecting CO_2 into the coal seam, CO_2 changes into different states: gaseous, subcritical, and supercritical. Due to the joint action of *in situ* stress, temperature, and the spatial deterioration of natural fractures, few studies have reported on the characteristics of the fracture mechanics in the coal seam. Coal has a clear bedding structure and anisotropic characteristics, which also affect its fracture properties. In particular, for bituminous coal rich in organic matter, supercritical CO_2 has a strong affinity for organic matter, making the situation even more complex and unknown. This highlights the need to consider both the CO_2 state and the anisotropy of the coal.

Currently, there is a lack of research on the effects of CO_2 state and coal anisotropy on the micro mechanisms involved in fracture mechanical properties, fracture trajectory, and macro mechanical behavior of bituminous coal. For bituminous coal rich in gas, there is more CO_2 displacement than CH_4, causing a more frequent mechanical response. This is a long-term process. Therefore, this study included a long-term CO_2 adsorption experiment, three-point bending fracture mechanics experiment, low-temperature nitrogen adsorption experiment, and fracture analysis of bituminous coal from an underground coal mine. These tests were performed to explore the influence of CO_2 state and anisotropy on the fracture characteristics, fracture trajectory, mineral dissolution, and action mechanisms associated with bituminous coal. The study quantitatively evaluated the changes in fracture mechanics parameters and microstructure of coal after CO_2 adsorption in different states, to better describe the underlying influencing mechanisms.

2 Experimental method and process

2.1 Sample preparation

The bituminous coal used in this study was collected from the Shenfu coalfield in Yulin, Shaanxi Province, China (Sun et al., 2022). The density of the bituminous coal is 1.23 g/cm^3. The uniaxial compressive strength measured by uniaxial compression test is 27.8 MPa in the horizontal bedding direction and 9.8 MPa in the vertical bedding direction. Table 1 presents the composition and content of the bituminous coal based on an industrial analysis (Sun et al., 2022). Here, M_{ad} indicates the moisture content on air-dried basis; V_{daf} refers to the volatile matter content; A_{ad} indicates the ash yield on air-dried basis; and FC_{ad} represents the fixed carbon content. Natural bituminous coal samples were collected from the mine. After removing the samples from the ground, they were immediately sealed with plastic wrap to retain their natural humidity characteristics.

Table 1 Industrial analysis of coal specimen

Sample	M_{ad}/%	A_{ad}/%	V_{daf}/%	FC_{ad}/%
Bituminous coal	7.00	6.68	31.54	54.78

According to standards recommended by the International Society for Rock Mechanics (ISRM) (Kuruppu et al., 2014), a semicircular bend (SCB) specimen was used to complete the fracture mechanics test experiment, with three types of constructed SCB samples, as shown in Fig. 1: crack-arrester type, crack-divider type, and crack-short transverse type. Bituminous coal has significant bedding, so three typical directions were selected to study the anisotropy of its mechanical properties.

In the same bituminous coal block, a cylinder was drilled perpendicular to the bedding plane, with a diameter of 50 mm along the bedding plane. Then, the cylinder was cut into a 20-mm thick disc, which was then cut into a half disc. The central straight crack length of the half disk was designed to align with the ISRM standard (Kuruppu et al., 2014). A 0.2 mm thick emery line was used to prefabricate a 12.5 mm straight cut groove in the center of the bottom of the half disc to form a standard SCB sample.

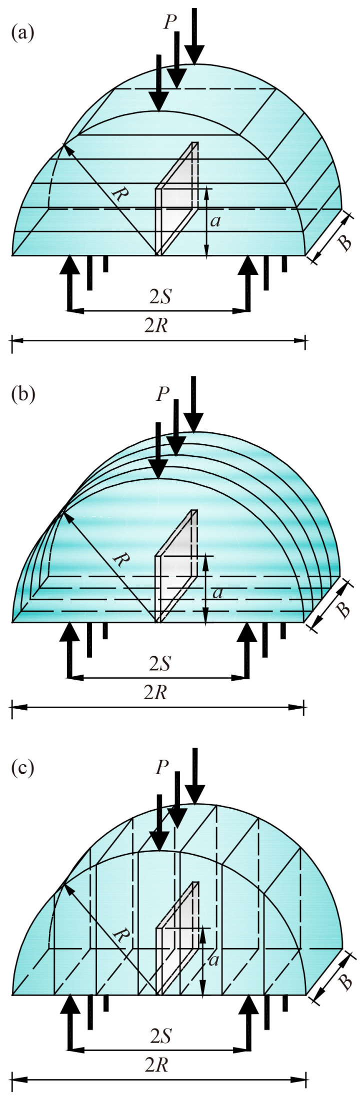

Fig. 1 Three SCB specimen types and loading diagram: *P*-Load (N); *B*-Specimen thickness (mm); *R*-Sample radius (mm); *a*-Prefabricated grooving length (mm); *S*-Span between two loading ends (mm). (a) Crack-arrester type; (b) Crack-divider type; (c) Crack-short transverse type.

2.2 CO_2 adsorption experiment

To explore the influence of CO_2 adsorption in different states on bituminous coal, four groups of CO_2 pressures were established: 4 MPa, 6 MPa, 8 MPa, and 12 MPa. The temperature was set to 40°C. At pressure levels of 4 MPa and 6 MPa, CO_2 is gaseous; at pressures of 8 MPa and 12 MPa, CO_2 is in a supercritical state. To fully saturate the bituminous coal sample and allow for sufficient reaction time, the adsorption time was set to 30 days. The experiment was conducted using an independently developed CO_2 adsorption device. The device (Sun et al., 2022), shown in Fig. 2, had four parts: vacuum-pumping system, compression and gas injection system, temperature and pressure control system, and reactor.

The experimental steps were as follows. 1) The bituminous coal samples were placed into the reactor and air was extracted for 24 h. This allowed the interior of the reactor and pipeline to approach a vacuum state. 2) The temperature control system was adjusted to slowly raise the temperature in the reactor to 40°C, at the heating rate of 1°C/min; the temperature was then held constant. 3) The CO_2 injection valve was opened suddenly to avoid damaging the flue gas injection system due to the slow increase in the CO_2 injection pressure. When the pressure in the reactor reached the set experimental value, the gas injection was stopped, and the system was monitored for 30 min to ensure that the temperature and pressure remained unchanged. This confirmed that the reactor was well sealed. 4) After the CO_2 had adsorbed into the bituminous coal samples in the reactor for 30 days, the pressure relief valve was opened to slowly discharge the CO_2 in the reactor. This reduced the pressure in the reactor to the atmospheric level. 5) The half disk bituminous coal samples were removed, wrapped with polyethylene film and sealed. The three-point bending fracture test immediately followed.

2.3 Fracture mechanics experiment

The three-point bending fracture test of the bituminous coal samples after CO_2 adsorption was conducted using an INSTRON 5544 experimental machine, shown in Fig. 3. The loading mode of constant displacement was adopted, with a loading rate of 0.0002 mm/s. During the experiment, the computer automatically recorded the load and displacement data.

Experimental data were analyzed and calculated using ISRM methods. The fracture toughness (K_{IC}) of SCB specimens was calculated using the following formula (Kuruppu et al., 2014):

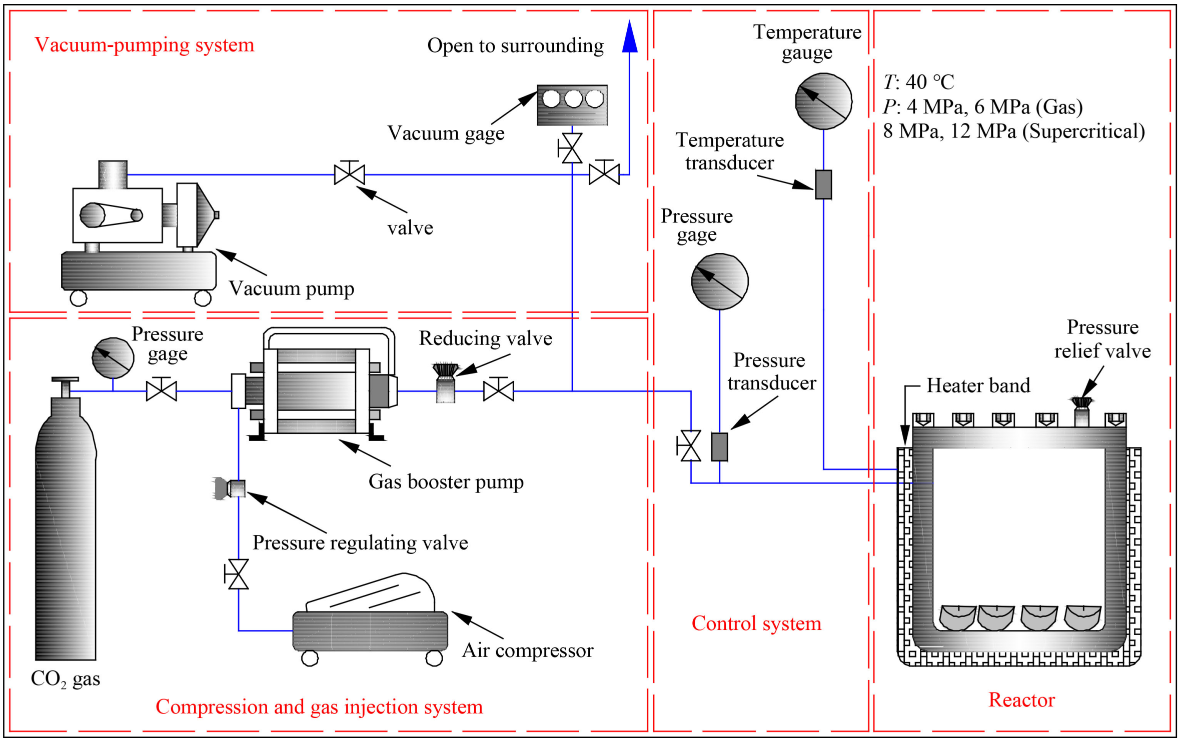

Fig. 2 Schematic diagram showing the CO_2 adsorption experimental system.

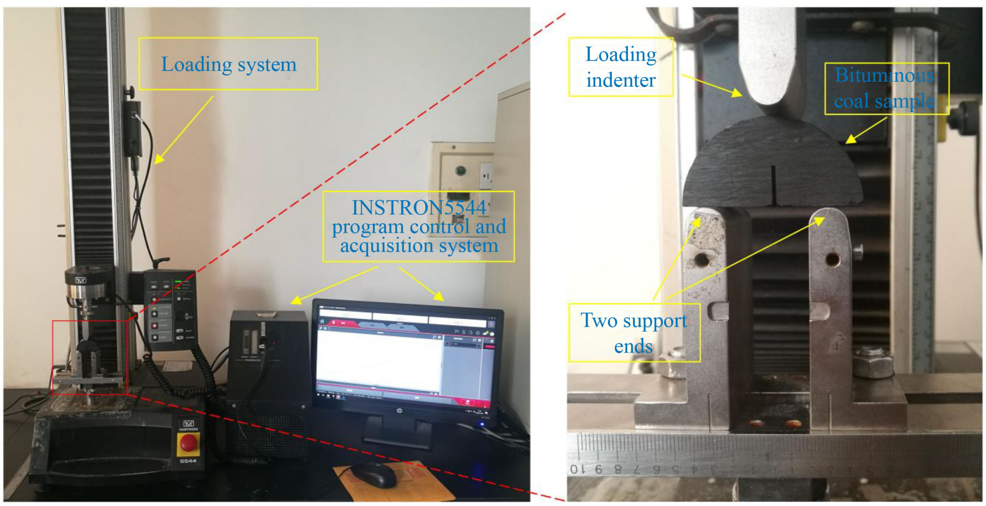

Fig. 3 Fracture mechanics experiment of bituminous coal SCB sample.

$$KIC = \frac{P_{max}\sqrt{\pi a}}{2RB}Y', \tag{1}$$

$$Y' = -1.297 + 9.516(2S/2R) - (0.47 + 16.457(2S/2R))\beta + (1.071 + 34.401(2S/2R))\beta^2, \tag{2}$$

$$\beta = a/R, \tag{3}$$

where P_{max} is the peak load of specimen failure; Y' is the dimensionless stress intensity factor; a/R is the ratio of the length of the prefabricated groove to the radius of the semicircular disk; and $2S$ is the span between two support ends. The sizes were as follows: $2S/(2R) = 0.61$, $a/R = 0.5$.

3 Mechanical experiment results and analysis

3.1 Fracture toughness of bituminous coal

Data were substituted into Eqs. (1)–(3) to calculate the mode-I fracture toughness of bituminous coal. Figure 4 plots the fracture toughness of bituminous coal sample against the CO_2 saturation pressure and bedding direction, based on the calculation results.

Figure 4(a) shows the changes in fracture toughness value for all bituminous coal samples with pressure. The mode-I fracture toughness of bituminous coal samples decreases to different degrees when CO_2 is adsorbed at different pressures. The maximum fracture toughness value of bituminous coal is 5.2396 MPa·mm$^{1/2}$; this is the value when there is no adsorption. When the CO_2 pressure is 4 MPa, the fracture toughness is 4.4294 MPa·mm$^{1/2}$, which is 15.5% lower compared to when there is no adsorption. When the CO_2 pressure increases to 6 MPa, the fracture toughness of bituminous coal samples decreases to 3.2740 MPa·mm$^{1/2}$, a decrease of 37.5%. When the pressure increases to 8 MPa, the fracture toughness is 1.9072 MPa·mm$^{1/2}$, which is 63.6% lower than that with no adsorption. This is the lowest value in the range evaluated. However, when the CO_2 saturation pressure increases to 12 MPa, the fracture toughness of bituminous coal is 4.1222 MPa·mm$^{1/2}$, which is 53.7% higher than that at the pressure of 8 MPa.

In summary, the fracture toughness of bituminous coal first decreases and then increases as the CO_2 pressure increases, with 8 MPa being the inflection point of this trend. Moreover, similar trends were also observed in the crack-arrester, crack-divider, and crack-short transverse type bituminous coal samples (Figs. 4(b)–4(d)). This may be because when the CO_2 saturation pressure exceeds a certain limit (8 MPa), the increased pore pressure leads to the compact compression of the matrix of bituminous coal (Pan and Connell, 2007; Chareonsuppanimit et al., 2014), which increases the fracture toughness. Ranjith and Perera (Ranjith and Perera, 2012; Perera et al., 2013; Ranathunga et al., 2016) tested the uniaxial compressive strength (UCS) of low rank coal under different CO_2 pressures and observed that UCS and elastic modulus (E) decreased with the increase in CO_2 saturation pressure.

Comparison of the fracture toughness of the three types of specimens indicates that they exhibit similar trends when the pressure changes. The fracture toughness is highest for the crack-divider type, followed by the crack-arrester type, followed by the crack-short transverse type. This is the case even under the same CO_2 pressure. The influence of bituminous coal bedding on its fracture mechanical properties is significant and deserves attention. In addition, the sensitivity of the fracture toughness of the three types of bituminous coal to CO_2 saturation pressure is different. There is a large fluctuation in the curves of the crack-arrester type and crack-divider type, while the curve fluctuation of the crack-short transverse type is small. Similar bedding studies on rock fracture toughness, including research by

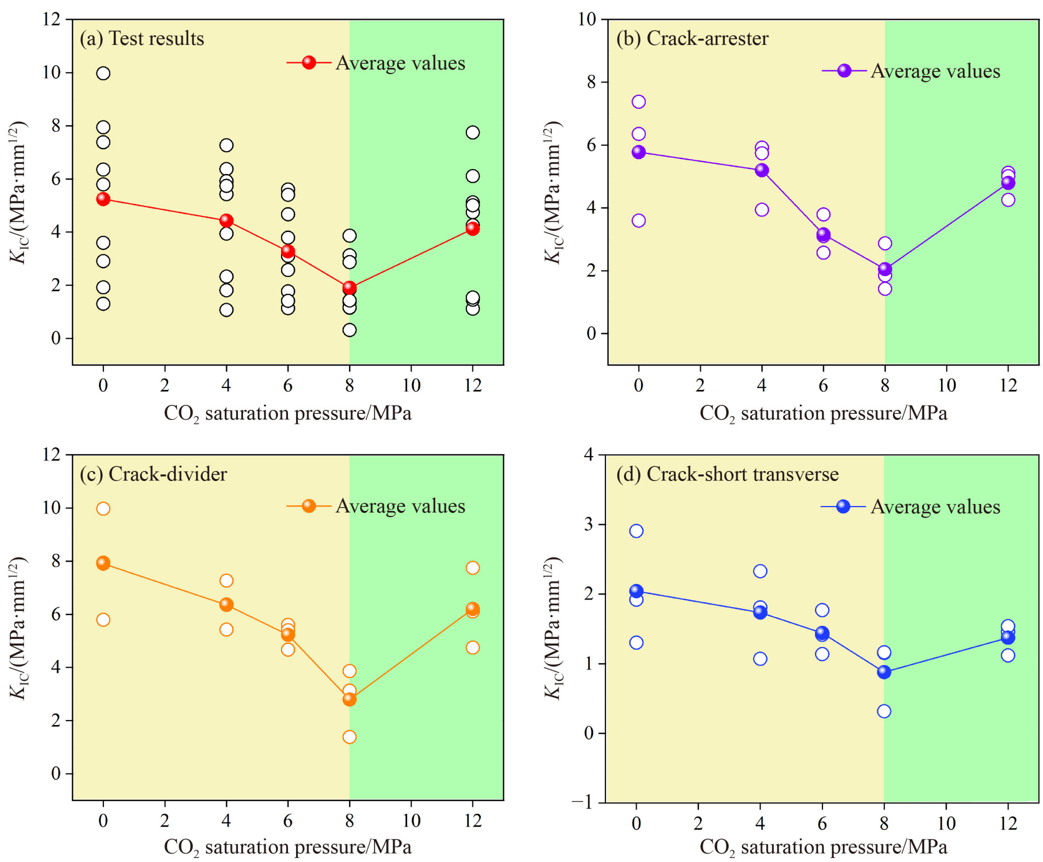

Fig. 4 Variation curve of mode-I fracture toughness of bituminous coal with CO_2 pressure.

Chandler et al. (2016), tested the mode-I fracture toughness of shale in three bedding directions. The results show there is significant anisotropy in the fracture toughness of shale. Of these, the mode-I fracture toughness of the crack-divider type is the highest and the fracture toughness of the crack-short transverse type is the lowest. To quantitatively illustrate the sensitivity of three types of bituminous coal samples to CO_2 saturation pressure, the anisotropy of fracture toughness is defined as

$$\gamma = K_{\mathrm{Imax}}/K_{\mathrm{Imin}}, \tag{4}$$

where K_{Imax} and K_{Imin} represent the maximum and minimum values, respectively, of bituminous coal fracture toughness in three bedding directions. The anisotropy of fracture toughness of bituminous coal sample is calculated using Eq. (4), as shown in Fig. 5.

Figure 5 shows that when the CO_2 saturation pressure increases from 4 MPa to 8 MPa, the anisotropy of bituminous coal fracture toughness gradually decreases to a minimum of 3.18. When the CO_2 saturation pressure rises to 12 MPa, the anisotropy of bituminous coal fracture toughness increases to 4.52. Therefore, the bedding of bituminous coal significantly influences its fracture toughness. Furthermore, the effect of bedding on the fracture toughness of bituminous coal depends on the CO_2 adsorption pressure. This dependence (anisotropy) is essentially the same as the changing trend of fracture toughness with CO_2 adsorption pressure.

3.2 Load–displacement curve

The load displacement curve can be obtained by the rock loading mechanics experiment, which is often used to analyze the mechanical characteristics of the rock failure process (Jin et al., 2020; Guo et al., 2021b; Hu et al., 2021; Zhang et al., 2021b; Li et al., 2022). Figure 6 shows the load displacement curve obtained during the three-point bending fracture experiment. Bituminous coal breaks after compaction and elastic and plastic deformation. The load displacement curves are similar for the bituminous coal sample with no adsorption and the sample undergoing 4 MPa CO_2 adsorption. The plastic stage is not significant, and all samples break suddenly upon reaching the peak load. The plastic deformation stage of bituminous coal is significant when the CO_2 pressure increases to 6 MPa. When the pressure reaches 8 MPa, bituminous coal gradually loses its stability and fractures after experiencing crack damage, showing a weakening in the brittleness. This is because the CO_2 adsorption gradually strengthens with the increase in pressure. When the CO_2 saturation pressure increases to 12 MPa, the plastic stage of bituminous coal is no longer significant, but the brittle fracturing property is somewhat enhanced. Therefore, the change in CO_2 pressure and phase state causes the bituminous coal to show the following characteristics during its transformation: “sudden fracture – gradual fracture – sudden fracture.”

Comparison of the load displacement curves of the three types of specimens shows significant differences. There is significantly less axial displacement of the crack-short transverse bituminous coal compared to the crack-arrester and crack-divider types. Therefore, the coal seam is subject to a loading mode that can easily lead to a lack of stability. This may be due to comprehensive factors such as the stress balance state and CO_2 corrosion of the matrix and bedding plane.

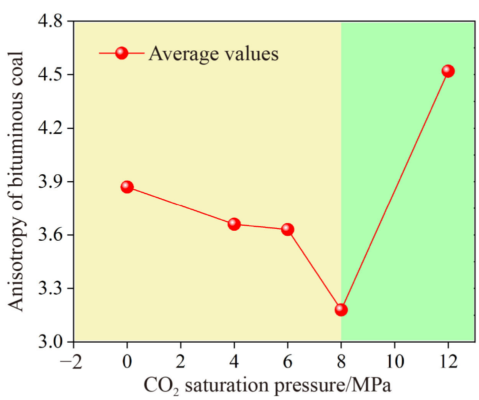

Fig. 5 Anisotropy of bituminous coal fracture toughness under different CO_2 pressures.

3.3 Fracture crack shape analysis

The rock’s fracture crack shape is determined by microscopic fracture mechanisms, and it directly reflects the fracture characteristics of rocks (Kataoka et al., 2015; Feng et al., 2017, 2018, 2020a, 2020b). Microscopic fractures reflect rock damage and also provide evidence explaining the rock’s ability to resist fracture. Changes in the mineral structure or the particle strength of the coal affect the growth path and development morphology of cracks. In addition to this, a weak plane structure and the heterogeneous characteristics of coal, such as bedding, cleat, and exogenous cracks, cause irregular fluctuations in the process of crack initiation and propagation along the tip. When testing the bituminous coal fracture toughness, the sample experiences fracture failure. The crack generally starts and expands along the tip of the prefabricated notch, gradually penetrating the sample. Figure 7 shows the typical fracture track and fracture surface of three types of bituminous coal samples.

It can be seen from Fig. 7 that the crack trajectories of the bituminous coal samples with the three bedding types are significantly different. The overall structure of the crack-arrester bituminous coal is broken, with a complex crack track. There are main cracks along the prefabricated notch direction, and secondary cracks along the weak bedding surface on the surface of most samples. The secondary cracks have different shapes, including: mode I

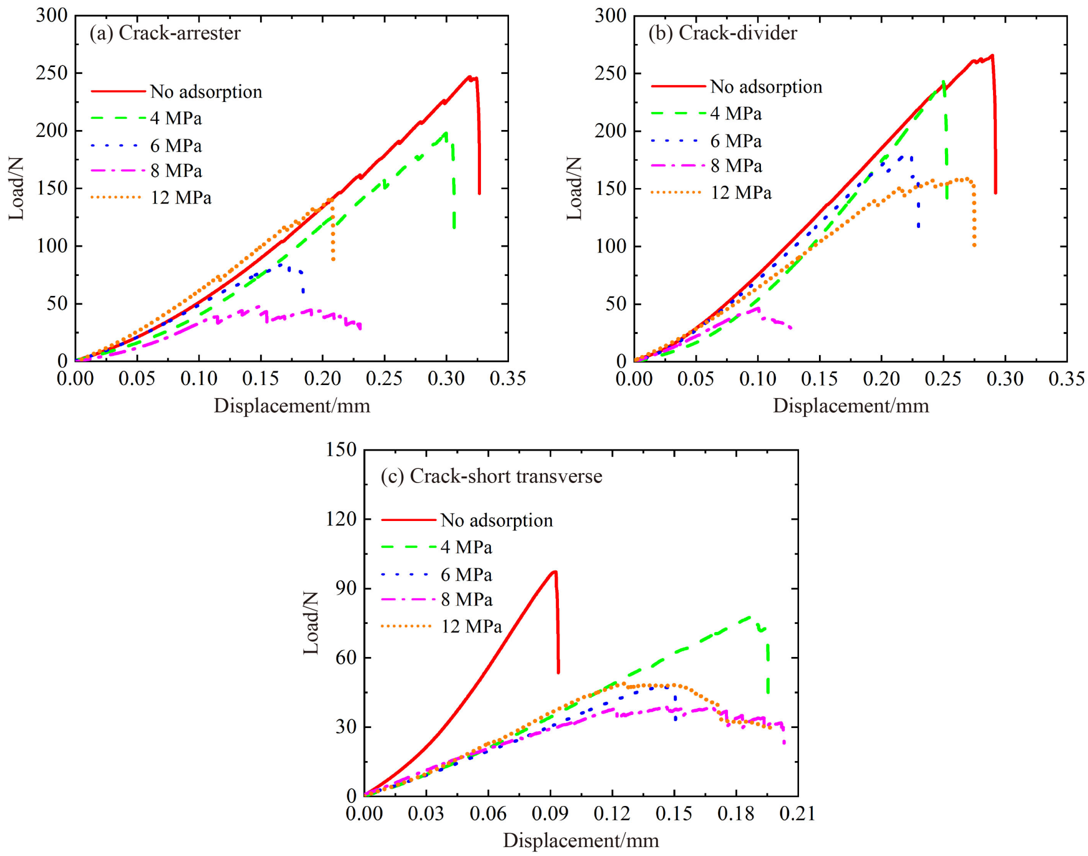

Fig. 6 Load displacement curve of bituminous coal during loading.

cracks that vertically pass through the bedding; intermittent cracks that turn at the weak surface and expand along the weak surface of the bedding; step cracks that expand a certain distance along the weak surface of the bedding and then turn again and continue to expand in the vertical direction of the bedding; and composite cracks that skew with the bedding.

The fracture morphology of the crack-arrester sample is rough (Fig. 7(a)). There is a significant bedding cracking phenomenon, with an irregular sawtooth shape. The overall structure of the crack-divider bituminous coal sample is relatively complete, and the geometric shape of the fracture track is similar to the crack-arrester type. However, there is a significant weakening in the stepped degree. The fracture track growth trajectory is mainly a single main crack, with few secondary cracks (Fig. 7(b)). The fracture surface of the sample is relatively flat, with few bedding cracks; however, there is a clear layered deposition of bituminous coal. The fracture track of the crack-arrester type mainly expands in the bituminous coal matrix. The crack-short transverse bituminous coal sample has a complete structure, and the fracture track propagation trajectory is a single main crack (Fig. 7(c)). The fracture track propagates along the tip of the prefabricated notch and its shape is essentially linear. The fracture surface is a weak bedding surface, which is relatively flat. The fracture track of the crack-short transverse bituminous coal is along the bedding plane.

4 Change in the pore structure of bituminous coal

The matrix of the bituminous coal provides its main bearing capacity. The coal's fracture properties are affected when the internal structure of the matrix changes. Coal is a porous and fractured source rock. The natural complex pore fracture system provides a migration channel for coalbed methane and a place to store geological CO_2. Within the pores of the bituminous coal, CO_2 undergoes complex physical and chemical reactions with the bituminous coal matrix over a long period of time. This changes the pore structure of the bituminous coal. Low-temperature nitrogen adsorption experiments were conducted on bituminous coal to test its specific surface area, total pore volume, and pore size distribution. Figure 8 shows the N_2 adsorption desorption isotherms of bituminous coal after adsorption under different CO_2 saturation pressures.

Using the BDDT classification (Brunauer et al., 1940), the N_2 adsorption desorption isotherms of the tested bituminous coal samples are classified as type IV, with

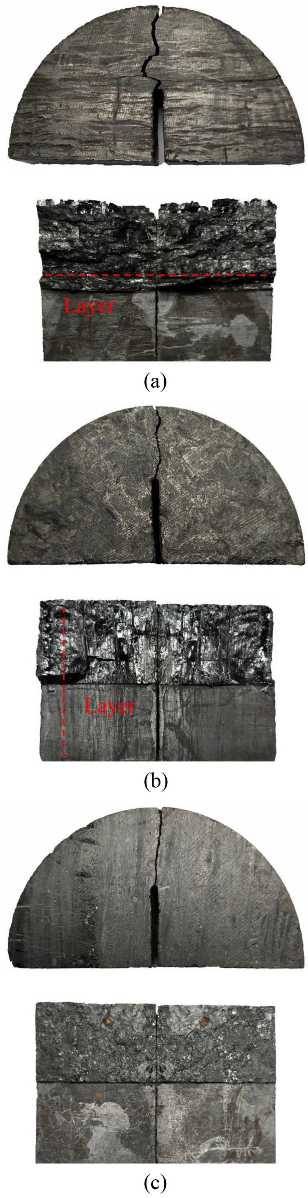

Fig. 7 Fracture track and fracture surface morphology of the three types of bituminous coal specimens. (a) Crack-arrester type; (b) crack-divider type; (c) crack-short transverse type.

clear hysteresis loops. The classification of the International Union of Pure and Applied Chemistry (IUPAC) (Brunauer et al., 1940; Sing et al., 1985) indicates that the hysteresis loop can be approximately classified as the H4 type; that is, the pore geometry in bituminous coal is mostly slit shaped pores. There is a small difference in the shape of the hysteresis loop associated with the isotherm of the bituminous coal samples, indicating that the change in CO_2 saturation pressure has little effect on the pore geometry of bituminous coal. The pore structure parameters of bituminous coal samples under different CO_2 saturation pressures were determined using adsorption isotherms according to the BET (Brunauer-Emmett-Teller) mode and Barrett-Joyner-Halenda (BJH) mode (Sing et al., 1985), as shown in Fig. 9.

Figure 9 shows that the specific surface area and total pore volume of the bituminous coal samples are lower after CO_2 adsorption compared to the samples without adsorption. As the pressure increases, the specific surface area and total pore volume first decrease and then increase; they reach the minimum value at 8 MPa and then slightly increase at 12 MPa. In contrast, the average pore size first increases and then decreases. There is also a clear effect of the interaction between bituminous coal and CO_2 on the pore size distributions. The nitrogen adsorption capacity reflects the adsorption capacity of bituminous coal. It can be seen that the adsorption capacity of bituminous coal decreases first and then increases with the change in CO_2 pressure, which is consistent with the change trend of specific surface area and total pore volume. In fact, after bituminous coal adsorbs CO_2, it suffers damage such as pores and cracks due to complex physicochemical reactions. Moreover, the volume of components contained in bituminous coal also expands, which may lead to the overall softening of bituminous coal.

The above result shows that the influence of CO_2 adsorption on the pore structure of bituminous coal differs in different CO_2 states. This phenomenon may be due to the dissolution of minerals and the extraction of hydrocarbons from coal caused by supercritical CO_2 adsorption (Agartan et al., 2015; Zhang et al., 2021c). There is a high level of organic matter in the pores of bituminous coal. The dissolution of organic matter by CO_2 injected into coal may cause pore expansion, and the pores are connected with each other to form larger pores, or even form fractures. This results in a reduced total number of pores. a smaller pore surface area, and an increase in the average size of the pores. However, as the pressure continues to rise, the proportion of micropores and mesopores does not decrease further. In contrast, the proportion of mesopores increases significantly, while the proportion of macropores decreases. The swelling caused by CO_2 adsorption may force macropores to change into mesopores. In addition, because the vitrinite of coal contains many pores, the content of the macerals of coal may also affect changes in the pores after interacting with supercritical CO_2 (Liu et al., 2022c).

Next, the complex changes in pore structure in the bituminous coal caused by CO_2 adsorption are further described. Based on the experimental results of the low-temperature nitrogen adsorption method, the fractal dimension calculation method of the Frenkel-Halsey-Hill (FHH) model proposed by Pfeiferper and Avnir (1983) is used to quantitatively describe the characteristic parameters of micropore structure of bituminous coal. The gas adsorbed on the fractal surface is expressed as (Avnir and Jaroniec, 1989)

$$\ln V = K\ln(\ln(p_0/p_1)) + C_1, \tag{5}$$

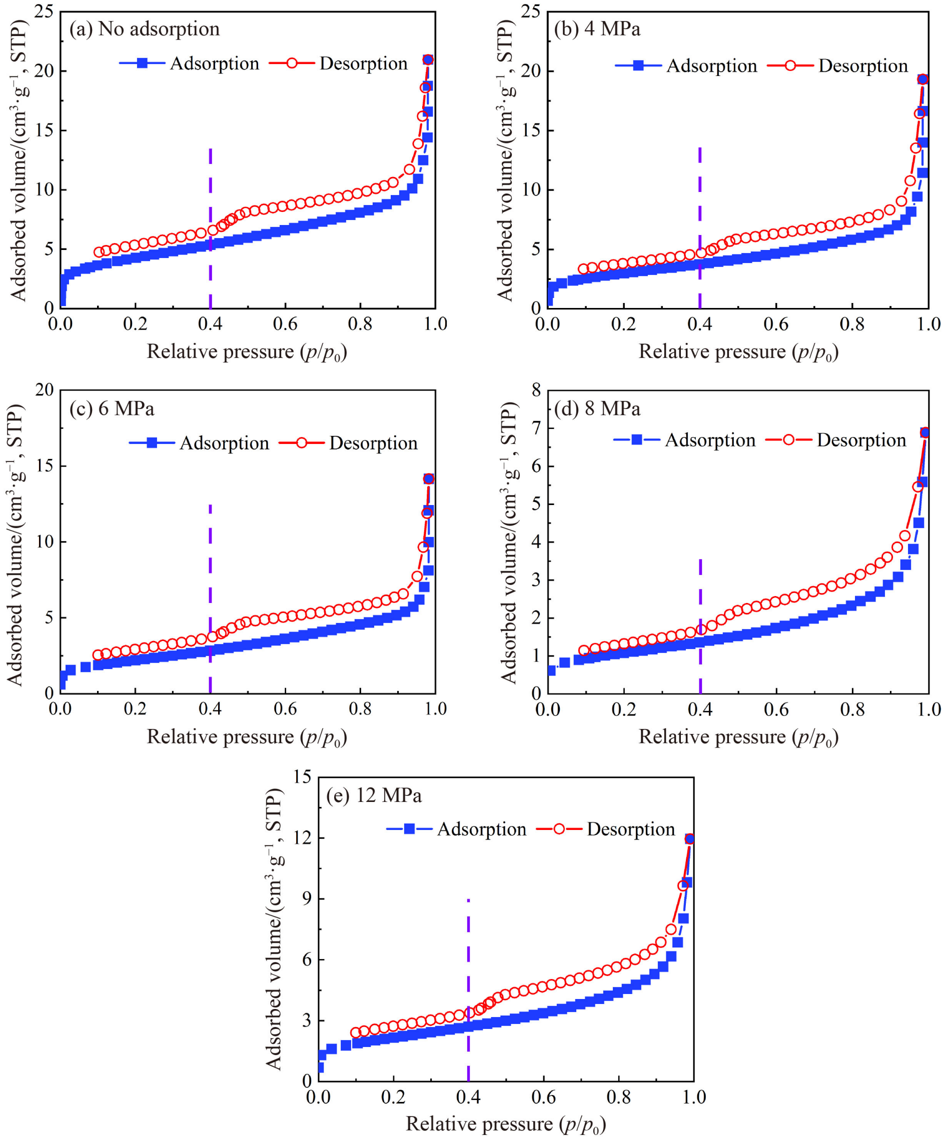

Fig. 8 Low temperature N_2 adsorption-desorption isotherms of bituminous coal samples (Sun et al., 2022).

$$D_1 = K + 3, \tag{6}$$

where V is the volume of adsorbed gas when the equilibrium pressure is p_1, cm^3/g; p_0 is the saturated vapor pressure, MPa; K is the slope; C_1 is a constant; and D_1 is a fractal dimension. Therefore, based on the N_2 isothermal adsorption data measured in the experiment, and using the fractal FHH model, Fig. 10 shows the linear relationship curve between $\ln V$ and $\ln(\ln(p_0/p_1))$. The fractal dimension (D_1) was calculated from the slope.

Figure 9 indicates that the bituminous coal sample experiences a hysteresis loop after the relative pressure exceeds 0.4. The adsorption branch and desorption branch of the isothermal adsorption line do not coincide, and the nitrogen adsorption only occurs in capillary condensation. Therefore, adsorption data with a relative pressure exceeding 0.4 are selected to further study the irregularity of the pore structure of bituminous coal under different CO_2 saturation pressures. Figure 10 shows that the correlation coefficients of the fitting curves exceed 0.97, indicating that bituminous coal has fractal characteristics. The fractal dimension of bituminous coal is between 2.6636–2.7666 (Table 2), and the pore surface and pore structure of bituminous coal are not uniform.

After CO_2 adsorption, the fractal dimension of bituminous coal sample slightly decreases, indicating that the pore surface roughness of bituminous coal decreases, and the pore structure gradually changes from being complex to being more regular. This is mainly because the organic matter in the bituminous coal is dissolved by CO_2, resulting in a reduced number of pores. The distribution of pore size tends to be simple, the pore structure is more uniform, and the complexity is reduced. However, this fractal feature is not prominent.

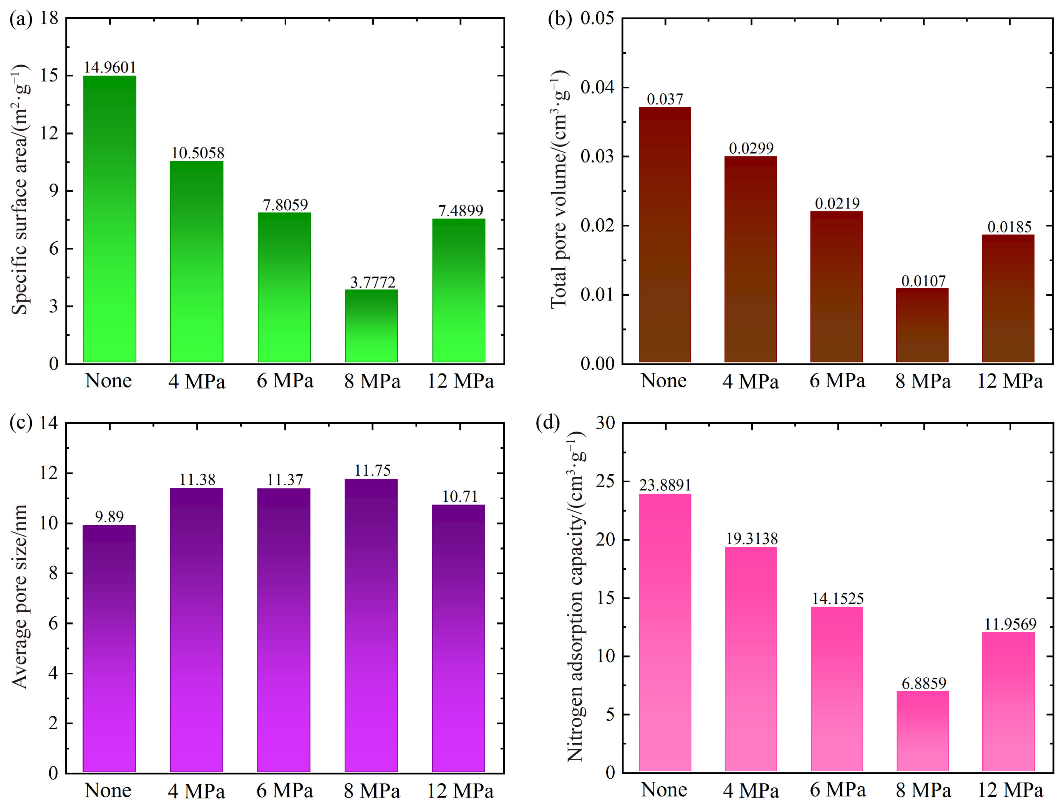

Fig. 9 Pore structure parameters of bituminous coal samples. (a) Specific surface area; (b) total pore volume; (c) average pore size; (d) nitrogen adsorption capacity (Modified from Sun et al., 2022).

5 Discussion

5.1 Effect of microscopic characteristics on fracture toughness of bituminous coal

Fracture toughness is a basic parameter of fracture mechanics used to measure the fracturing resistance of materials. It is affected by pore structure characteristics. To clearly observe the relationship between the fracture toughness of bituminous coal and pore structure parameters, Fig. 11 shows the microscopic characteristic parameters of bituminous coal, the fracture toughness of bituminous coal in the same coordinate system, and the correlation between them.

Phenomenologically, Fig. 11 shows that the changing trend of surface area and fracture toughness of bituminous coal remains essentially the same with change in CO_2 pressure; both first decrease and then increase. The changing trend of total pore volume and fracture toughness of bituminous coal with CO_2 pressure is also essentially the same; it first decreases and then increases. The volume expansion of bituminous coal is also large due to CO_2 adsorption, and the bituminous coal becomes soft as a whole. However, the average pore size first increases and then decreases with the increase in CO_2 adsorption pressure. This result is opposite to the changing trend of fracture toughness. After adsorbing CO_2, the ability of bituminous coal to adsorb gas also changes, and the change trend is consistent with that of fracture toughness. However, the low-temperature nitrogen adsorption experiment can only test the pores within a certain size range. How the pores beyond this range affect the mechanical properties needs further research.

Moreover, the turning point of the changing trend with respect to specific surface area, total pore volume, average pore diameter, and fracture toughness is 8 MPa. Phenomenally, there is a positive correlation between specific surface area, total pore volume, and fracture toughness. In contrast, there is a negative correlation between average pore size and fracture toughness. This may be related to the mutual transformation between macropores and mesopores. The complex physical and chemical reactions between CO_2 and the organic matter and minerals contained in bituminous coal lead to the change in pore structure. On the other hand, the pore structure of bituminous coal affects its fracture mechanical properties. Especially under the influence of 8 MPa supercritical CO_2, the pore change of bituminous coal is the most obvious, which directly leads to its loose structure, reduces the interaction force between molecules, and weakens the ability of bituminous coal to resist fracture (fracture toughness). Moreover, some closed pores are transformed into open pores, while others become dense due to the adsorption of precipitated materials. This process is very complex, accompanied by

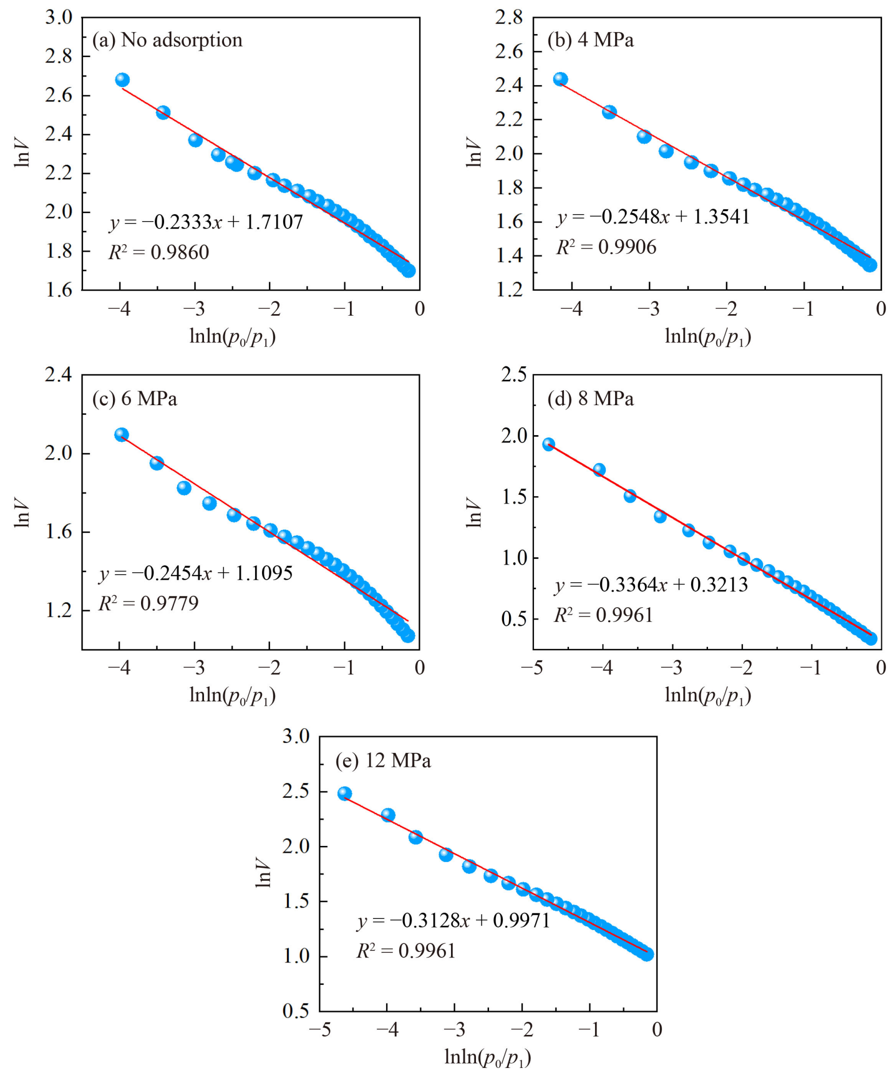

Fig. 10 Plots of ln$V$ vs lnln(p_0/p_1) from N_2 adsorption data.

Table 2 Fractal dimension of bituminous coal samples under different CO_2 pressures in the FHH model

Pressure/MPa	0	4	6	8	12
D_1	2.7667	2.7452	2.7546	2.6636	2.6872

the transformation between micropores, mesopores and macropores.

Some studies have shown that the changes in mechanical properties caused by CO_2 adsorption of coal are reversible under certain conditions, that is, after CO_2 is desorbed, the mechanical properties of coal can be partially restored (Masoudian et al., 2014). This largely depends on the state of CO_2 when it interacts with coal, that is, the CO_2 action in gaseous state, subcritical state and supercritical state. The reversibility of mechanical properties of bituminous coal is different. Liu et al. (2022c) found a negative correlation between the specific surface area of coal and the uniaxial compressive strength when studying the effect of adsorption time on the strength of anthracite. For bituminous coal rich in organic matter, the complex composition and structure lead to complex changes in its internal pore structure after CO_2 adsorption. This change may differ for anthracite. Contrary results are seen when examining the influence of changes in the internal pores of bituminous coal and anthracite on their respective mechanical characteristics. This also shows that when studying the influence of CO_2 adsorption on the macro mechanical behavior of coal, it is critical to consider distinctions between different coal types.

5.2 Influence of CO_2 on bituminous coal

The physicochemical effect of CO_2 on coal is very complex. The above results show that the pore structure of bituminous coal is altered, which causes changes in the fracture characteristics of bituminous coal. On the one hand, these results are related to the chemical reaction of CO_2 corrosion of coal. On the other hand, CO_2 adsorption

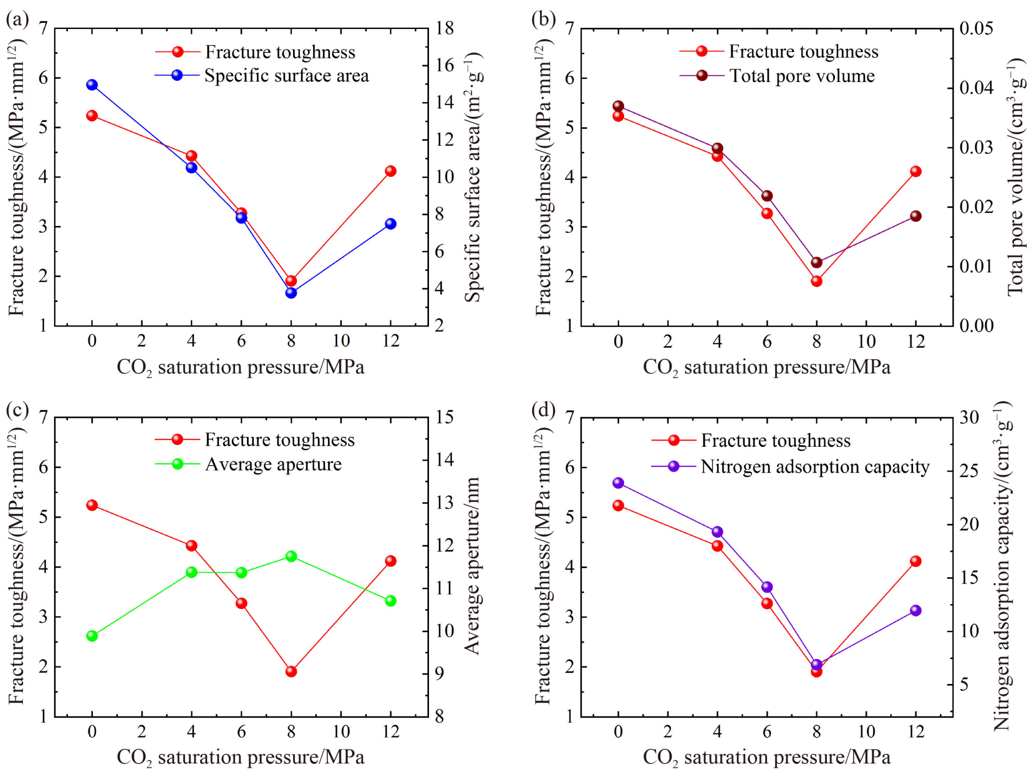

Fig. 11 Relationship curve between fracture toughness and pore structure parameters for bituminous coal: (a) comparison of fracture toughness and specific surface area; (b) comparison of fracture toughness and total pore volume; (c) comparison of fracture toughness and average aperture; (d) comparison of fracture toughness and nitrogen a dsorption capacity.

is related to the physical and mechanical effects caused by coal. It is reported that mineral components in coal are mainly comprised of calcite, clay mineral, quartz, dolomite, aragonite, pyrite, and siderite (Mandile and Hutton, 1995). In the acidic environment formed by CO_2 dissolution in water, complex chemical reactions can occur for the mineral components contained in coal. This acidic environment can lead to the dissolution and precipitation of minerals in coal, especially the dissolution of carbonate minerals, which directly leads to the change in coal pore structure. In particular, supercritical CO_2 is a good organic solvent, which has a significant impact on bituminous coal with high organic content. Studies have shown that the change in pore structure is irreversible (Liu et al., 2022c), more and more weak interfaces are produced, and fracture crack propagation occurs with loading.

In addition, the differential expansion caused by CO_2 adsorption between different coal types is also the cause of internal stress in coal (Chen et al., 2022; Kong et al., 2022) have shown that the transition from glassy solid state to rubber state can explain the expansion process accompanying CO_2 adsorption. Masoudian et al. (2013 and 2014) found through experimental research that CO_2 adsorption can destroy the coal structure, expand, soften and weaken it. The adsorption of CO_2 changes the elastic modulus and strength of coal samples, and these effects are reversible. Therefore, they concluded that the changes in mechanical properties and microstructure of coal caused by adsorption were similar to the effects of plasticizers on polymers (Feng et al., 2019). From the above analysis, it can be seen that the structure of bituminous coal changes due to complex physical and chemical effects, which leads to the change in its ability to resist fracture.

5.3 Effect of bedding on fracture characteristics of bituminous coal

By analyzing the fracture track geometry and fracture morphology of three different bedding types of bituminous coal, it was found that the anisotropy associated with the fracture toughness of bituminous coal is mainly caused by the anisotropy of the toughening mechanism during the propagation of the fracture track. For a layered sedimentary rock such as bituminous coal, there are three main toughening mechanisms in the fracture process: the weak surface cracking of the bedding, the deviation of the fracture path, and delamination stripping (Heng et al., 2015). If there are multiple toughening mechanisms, bituminous coal may have stronger fracture toughness.

The crack-short transverse bituminous coal sample breaks when subjected to an external load. The low cementation strength of the bedding surface leads to weakness, or a low ability to prevent the propagation of fracture trajectories. According to the Maximum Tangential Stress criterion (Heng et al., 2015; Feng et al., 2020a, 2020b), when the maximum circumferential stress at the crack tip exceeds the tensile strength of the weak bedding plane, the crack propagates along the direction of the original mode I crack. During the fracture process, the fracture track starts and expands along the artificial notch tip and the weak bedding plane. There is no deflection of the fracture path and delamination. Only the weak bedding plane cracks, which is a toughening mechanism, and the bedding plane shows a relatively flat crack geometry, as displayed in Fig. 7(c). Therefore, the three-point bending fracture test revealed that this type of bituminous coal has the smallest fracture toughness value. The crack-divider bituminous coal sample is subjected to the load, and the fracture track starts to crack along the prefabricated crack tip and propagates through the matrix. Then, the fracture path gradually deviates from the prefabricated notch direction, increasing the propagation path. The mechanical structure shows that the fracture trajectory is orthogonal to and passes through the weak bedding plane. The cementation strength of the weak bedding plane is significantly smaller compared to the coal matrix. As such, the tensile stress perpendicular to the weak bedding plane peels off the weak bedding plane due to the stress generated by the load at the crack tip, as shown in Fig. 12.

The generation and development of layer peeling has a crack arrest effect, and can cause the sample crack to create multiple lamellar structures. The separation between lamellar structures transforms the main crack propagation into multiple simultaneous and parallel discontinuous cracks. The stress state at the front of these cracks changes from three-dimensional stress to plane strain, inhibits the deformation of bituminous coal, increases the crack propagation resistance, and macroscopically shows the enhanced toughness of bituminous coal. This increases fracture resistance. The results of this study revealed that the fracture toughness of the loading types of bituminous coal is highest for the crack-divider type, followed by the crack-arrester type, followed by the crack-short transverse type. However, Wu et al. (2017) studied the mode-I fracture characteristics of coal body in different bedding directions, and showed that the K_{IC} value of the crack-arrester type exceeded that of the crack-divider type. The relative fracture toughness of crack-arrester and crack-divider bituminous coal samples is closely related to the strength of layered material matrix and the degree of interlayer peeling (Heng et al., 2015).

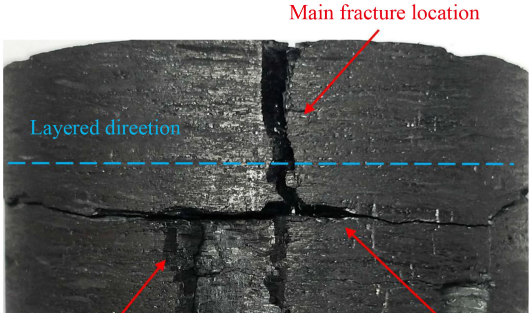

Fig. 12 Delamination phenomenon of crack-divider bituminous coal sample.

6 Conclusions

This study focused on CO_2 adsorption in bituminous coal, and included CO_2 adsorption experiments, fracture mechanics experiments and low-temperature nitrogen adsorption experiments. The effects of the CO_2 state during adsorption and bedding direction on the fracture characteristics of bituminous coal were studied based on analysis and discussion of the experimental data. The main study conclusions are as follows.

1) Sub-/super-critical CO_2 has significant impact on bituminous coal fracture mechanical properties. The K_{IC} of bituminous coal first decreases and then increases as the CO_2 saturation pressure increases. Especially, when the CO_2 pressure is 8 MPa, the K_{IC} decreases the most (63.6% lower than that without adsorption). This may be due to the compression of the coal based body caused by higher pressure. The instability characteristics of bituminous coal show the transformation trend of “sudden fracture - gradual fracture - sudden fracture.”

2) Bituminous coal samples display different abilities to resist mode-I crack propagation along the parallel bedding orientation, vertical bedding orientation, and orthogonal bedding orientation. CO_2 adsorption does not change the order of K_{IC} (crack-divider type > crack-arrester type > crack-short transverse type). The nonuniform change in pore structure caused by CO_2 adsorption affects the fracture toughness of these three types of bituminous coal samples.

3) The fracture trajectory of bituminous coal shows significant anisotropy. The crack-arrester type fracture trajectory presents a multi-branch and ladder shape. The fracture track of the crack-short transverse type and the crack-divider type bituminous coal is relatively singular, mainly extending along the direction of the prefabricated groove. The above results could be due to the inconsistent stress of the bituminous coal under different loading modes. Furthermore, there are significant differences in the mechanical strength of the bedding plane and matrix of bituminous coal. In particular, when there are different CO_2 adsorption states, the differences in the mechanical characteristics between the bedding plane and the bituminous coal matrix become more significant.

4) The change in the pore structure of bituminous coal differs under different CO_2 adsorption pressures, with a

significant effect on the fracture toughness of bituminous coal. The specific surface area and total pore volume of bituminous coal are positively correlated with fracture toughness. In contrast, the average pore size of bituminous coal is negatively correlated with fracture toughness. The change in fracture characteristics of bituminous coal depends on the CO_2 adsorption state, which may be related to mineral dissolution in coal, organic matter extraction, and the mutual transformation between pores with different pore sizes.

Acknowledgments This study has been partially funded by Youth Program of National Natural Science Foundation of China (Grant No. 51904195) and the School Fund of Taiyuan University of Technology and Science (No. 20182008). These supports are gratefully acknowledged.

References

Agartan E, Trevisan L, Cihan A, Birkholzer J, Zhou Q L, Illangasekare T H (2015). Experimental study on effects of geologic heterogeneity in enhancing dissolution trapping of supercritical CO_2. Water Resour Res, 51(3): 1635–1648

Avnir D, Jaroniec M (1989). An isotherm equation for adsorption on fractal surface of heterogeneous porous materials. Langmuir, 5(6): 1431–1433

Brunauer S, Deming L S, Deming W S, Teller E (1940). On a theory of the van der Waals adsorption of gases. J Am Chem Soc, 62(7): 1723–1732

Chandler M R, Meredith P G, Brantut N, Crawford B R (2016). Fracture toughness anisotropy in shale. J Geophys Res Solid Earth, 121(3): 1706–1729

Chareonsuppanimit P, Mohammad S A, Robinson R L, Gasem K A M (2014). Modeling gas-adsorption induced swelling and permeability changes in coals. Int J Coal Geol, 121: 98–109

Chen K, Liu X F, Nie B S, Zhang C P, Song D Z, Wang L K, Yang T (2022). Mineral dissolution and pore alteration of coal induced by interactions with supercritical CO_2. Energy, 248: 123627

Chen T Y, Feng X T, Zhang X W, Cao W D, Fu C J (2014). Experimental study on mechanical and anisotrpic properties of black shale. Chin J Rock Mech Eng, 33 (9): 1772–1779 (in Chinese)

Cheng L, Li D, Wang W, Liu J (2021). Heterogeneous transport of free CH_4 and free CO_2 in dual-porosity media controlled by anisotropic in situ stress during shale gas production by CO_2 flooding: implications for CO_2 geological storage and utilization. ACS Omega, 6(40): 26756–26765

Czerw K, Baran P, Szczurowski J, Zarębska K (2021). Sorption and desorption of CO_2 and CH_4 in vitrinite- and inertinite-rich polish low-rank coal. Nat Resour Res, 30(1): 543–556

Farmer I W, Pooley F D (1967). A hypothesis to explain the occurrence of outbursts in coal, based on a study of West Wales outburst coal. Int J Rock Mech Min Sci Geomech Abstr, 4(2): 189–193

Feng G, Kang Y, Chen F, Liu Y W, Wang X C (2018). The influence of temperature on mixed-mode (I+II) and mode-II fracture toughness of sandstone. Eng Fract Mech, 189: 51–63

Feng G, Kang Y, Meng T, Hu Y Q, Li X H (2017). The influence of temperature on mode I fracture toughness and fracture characteristics of sandstone. Rock Mech Rock Eng, 50(8): 2007–2019

Feng G, Kang Y, Sun Z D, Wang X C, Hu Y Q (2019). Effects of supercritical CO_2 adsorption on the mechanical characteristics and failure mechanisms of shale. Energy, 173: 870–882

Feng G, Kang Y, Wang X C, Hu Y Q, Li X H (2020c). Investigation on the failure characteristics and fracture classification of shale under Brazilian test conditions. Rock Mech Rock Eng, 53(7): 3325–3340

Feng G, Wang X C, Kang Y, Zhang Z T (2020a). Effect of thermal cycling-dependent cracks on physical and mechanical properties of granite for enhanced geothermal system. Int J Rock Mech Min Sci, 134: 104476

Feng G, Wang X C, Wang M, Kang Y (2020b). Experimental investigation of thermal cycling effect on fracture characteristics of granite in a geothermal-energy reservoir. Eng Fract Mech, 235: 107180

Gao M Z, Xie J, Gao Y N, Wang W Y, Li C, Yang B G, Liu J J, Xie H P (2021). Mechanical behavior of coal under different mining rates: a case study from laboratory experiments to field testing. Int J Min Sci Technol, 31(5): 825–841

Gao M Z, Zhang J G, Li S W, Wang M, Wang Y W, Cui P F (2020). Calculating changes in fractal dimension of surface cracks to quantify how the dynamic loading rate affects rock failure in deep mining. J Cent South Univ, 27(10): 3013–3024

Guo P Y, Gu J, Su Y, Wang J, Ding Z W (2021b). Effect of cyclic wetting–drying on tensile mechanical behavior and microstructure of clay-bearing sandstone. Int J Coal Sci Technol, 8(5): 956–968

Guo Y X, Zhao Y H, Wang S W, Feng G R, Zhang Y J, Ran H Y (2021a). Stress-strain-acoustic responses in failure process of coal rock with different height to diameter ratios under uniaxial compression. J Cent South Univ, 28(6): 1724–1736

Hedges S W, Soong Y, Jones J R M, Harrison D K, Irdi G, Frommell E, Dilmore R, White C (2007). Exploratory study of some potential environmental impacts of CO_2 sequestration in unmineable coal seams. Int J Environ Pollut, 29(4): 457–473

Heng S, Yang C H, Guo Y T, Wang C Y, Wang L (2015). Influence of bedding planes on hydraulic fracture propagation in shale formations. Chin J Rock Mech Eng, 34 (2): 228–237 (in Chinese)

Hou L L, Liu X J, Liang L X, Xiong J, Zhang P, Xie B, Li D Q (2020). Investigation of coal and rock geo-mechanical properties evaluation based on the fracture complexity and wave velocity. J Nat Gas Sci Eng, 75: 103133

Hu J J, Xie H P, Sun Q, Li C B, Liu G K (2021). Changes in the thermodynamic properties of alkaline granite after cyclic quenching following high temperature action. Int J Min Sci Technol, 31(5): 843–852

Jin J F, Yuan W, Wu Y, Guo Z Q (2020). Effects of axial static stress on stress wave propagation in rock considering porosity compaction and damage evolution. J Cent South Univ, 27(2): 592–607

Kataoka M, Obara Y, Kuruppu M (2015). Estimation of fracture toughness of anisotropic rocks by semi-circular bend (SCB) tests under water vapor pressure. Rock Mech Rock Eng, 48(4): 1353–1367

Keboletse K P, Ntuli F, Oladijo O P (2021). Influence of coal properties on coal conversion processes-coal carbonization, carbon fiber production, gasification and liquefaction technologies: a review. Int J Coal Sci Technol, 8(5): 817–843

Kong X G, He D, Liu X F, Wang E Y, Li S G, Liu T, Ji P F, Deng D Y, Yang S R (2022). Strain characteristics and energy dissipation laws of gas-bearing coal during impact fracture process. Energy, 242: 123028

Kuruppu M D, Obara Y, Ayatollahi M R, Chong K P, Funatsu T (2014). ISRM-suggested method for determining the mode I static fracture toughness using semi-circular bend specimen. Rock Mech Rock Eng, 47(1): 267–274

Lampert A (2019). Over-exploitation of natural resources is followed by inevitable declines in economic growth and discount rate. Nat Commun, 10(1): 1419

Li Y J, Song L H, Tang Y J, Zuo J P, Xue D J (2022). Evaluating the mechanical properties of anisotropic shale containing bedding and natural fractures with discrete element modeling. Int J Coal Sci Technol, 9(1): 18

Liao Z W, Liu X F, Song D Z, He X Q, Nie B S, Yang T, Wang L K (2021). Micro-structural damage to coal induced by liquid CO_2 phase change fracturing. Nat Resour Res, 30(2): 1613–1627

Liu B, Zhao Y X, Zhang C, Zhou J L, Li Y T, Sun Z (2021a). Characteristic strength and acoustic emission properties of weakly cemented sandstone at different depths under uniaxial compression. Int J Coal Sci Technol, 8(6): 1288–1301

Liu C R, Tang Y F, Wang H Q, Liu Z Q, Yang S, Li C J, Jin W T (2022a). Comparison of life cycle performance of distributed energy system and conventional energy system for district heating and cooling in China. J Cent South U, 29(7): 2357–2376

Liu J, Xie L, Elsworth D, Gan Q (2019a). CO_2/CH_4 competitive adsorption in shale: implications for enhancement in gas production and reduction in carbon emissions. Environ Sci Technol, 53(15): 9328–9336

Liu J, Yao Y, Liu D, Elsworth D (2017). Experimental evaluation of CO_2 enhanced recovery of adsorbed-gas from shale. Int J Coal Geol, 179: 211–218

Liu K D, Liu Q S, Zhu Y G(2013). Experimental study of coal considering directivity effect of bedding plane under Brazilian splitting and uniaxial compression. Chin J Rock Mech Eng, 32: 308–315 (in Chinese)

Liu S M, Li X L, Wang D K, Zhang D M (2021b). Experimental study on temperature response of different ranks of coal to liquid nitrogen soaking. Nat Resour Res, 30(2): 1467–1480

Liu X F, Nie B S (2016). Fractal characteristics of coal samples utilizing image analysis and gas adsorption. Fuel, 182: 314–322

Liu X F, Song D Z, He X Q, Nie B S, Wang L K (2019c). Insight into the macromolecular structural differences between hard coal and deformed soft coal. Fuel, 245: 188–197

Liu X F, Wang L K, Kong X G, Ma Z T, Nie B S, Song D Z, Yang T (2022d). Role of pore irregularity in methane desorption capacity of coking coal. Fuel, 314: 123037

Liu X F, Zhang C L, Nie B S, Zhang C P, Song D Z, Yang T, Ma Z T (2022c). Mechanical response and mineral dissolution of anthracite induced by supercritical CO_2 saturation: influence of saturation time. Fuel, 319: 123759

Liu X, Song D, He X, Wang Z, Zeng M, Deng K (2019b). Nanopore structure of deep-burial coals explored by AFM. Fuel, 246: 9–17

Liu Z Y, Wang G, Li J Z, Li H X, Zhao H F, Shi H W, Lan J L (2022b). Water-immersion softening mechanism of coal rock mass based on split Hopkinson pressure bar experiment. Int J Coal Sci Technol, 9(1): 61

Ma Q, Tan Y L, Liu X S, Zhao Z H, Fan D Y, Purev L (2021). Experimental and numerical simulation of loading rate effects on failure and strain energy characteristics of coal-rock composite samples. J Cent South U, 28(10): 3207–3222

Mabuza M, Premlall K, Daramola M O (2022). Modelling and thermodynamic properties of pure CO_2 and fue gas sorption data on South African coals using Langmuir, Freundlich, Temkin, and extended Langmuir isotherm models. Int J Coal Sci Technol, 9(1): 45

Mandile A J, Hutton A C (1995). Quantitative X-ray diffraction analysis of mineral and organic phases in organic-rich rocks. Int J Coal Geol, 28(1): 51–69

Masoudian M S, Airey D W, El-Zein A (2013). A chemo-poro-mechanical model for sequestration of carbon dioxide in coalbeds. Geotechnique, 63(3): 235–243

Masoudian M S, Airey D W, El-Zein A (2014). Experimental investigations on the effect of CO_2 on mechanics of coal. Int J Coal Geol, 128–129: 12–23

Nikolenko P V, Epshtein S A, Shkuratnik V L, Anufrenkova P S (2021). Experimental study of coal fracture dynamics under the influence of cyclic freezing–thawing using shear elastic waves. Int J Coal Sci Technol, 8(4): 562–574

Niu Q H, Cao L W, Sang S X, Wang W, Zhou X Z, Yuan W, Ji Z M, Chang J F, Li M Y (2021). Experimental study on the softening effect and mechanism of anthracite with CO_2 injection. Int J Rock Mech Min Sci, 138: 104614

Niu Q, Cao L, Sang S, Zhou X, Wang W, Yuan W, Ji Z M, Wang H C, Nie Y (2020). Study on the anisotropic permeability in different rank coals under influences of supercritical CO_2 adsorption and effective stress and its enlightenment for CO_2 enhance coalbed methane recovery. Fuel, 262: 116515

Omotilewa O J, Panja P, Vega-Ortiz C, McLennan J (2021). Evaluation of enhanced coalbed methane recovery and carbon dioxide sequestration potential in high volatile bituminous coal. J Nat Gas Sci Eng, 91: 103979

Pan Z J, Connell L D (2007). A theoretical model for gas adsorption-induced coal swelling. Int J Coal Geol, 69(4): 243–252

Patel M J, May E F, Johns M L (2016). High-fidelity reservoir simulations of enhanced gas recovery with supercritical CO_2. Energy, 111: 548–559

Perera M S A, Ranjith P G, Viete D R (2013). Effects of gaseous and super-critical carbon dioxide saturation on the mechanical properties of bituminous coal from the Southern Sydney Basin. Appl Energy, 110: 73–81

Pfeiferper P, Avnir D (1983). Chemistry in noninteger dimensions between two and three. I. Fractal theory of heterogeneous surfaces. J Chem Phys, 79(7): 3558–3565

Qiu L M, Liu Z T, Wang E Y, He X Q, Feng J J, Li B L (2020). Earlywarning of rock burst in coal mine by lowfrequency electromagnetic radiation. Eng Geol, 279: 105755

Ranathunga A S, Perera M S A, Ranjith P G, Bui H (2016). Super-critical CO_2 saturation-induced mechanical property alterations in low rank coal: an experimental study. J Supercrit Fluids, 109: 134–140

Ranjith P G, Perera M S A (2012). Effects of cleat performance on strength reduction of coal in CO_2 sequestration. Energy, 45(1): 1069–1075

Raza A, Gholami R, Rezaee R, Rasouli V, Rabiei M (2019). Significant aspects of carbon capture and storage – a review. Petroleum, 5(4): 335–340

Say N P, Yücel M (2006). Energy consumption and CO_2 emissions in Turkey: empirical analysis and future projection based on an economic growth. Energy Policy, 34(18): 3870–3876

Sing K S W, Everett D H, Haul R A W, Moscou L, Pierotti R A, Rouquerol J, Siemieniewska T (1985). Reporting physisorption data for gas/solid systems with special reference to the determination of surface area and porosity. Pure Appl Chem, 57(4): 603–619

Souley Agbodjan Y, Liu Z, Wang J, Yue C, Luo Z (2022). Modeling and optimization of a multi-carrier renewable energy system for zero-energy consumption buildings. J Cent South U, 29(7): 2330–2345

Sun Z D, Feng G, Song X M, Meng T, Zhu D F, Huo Y M, Wang Z L (2022). Effects of CO_2 state and anisotropy on the progressive failure characteristics of bituminous coal: an experimental study. Chin J Rock Mech Eng, 41(11): 70–81 (in Chinese)

Tan L H, Ren T, Yang X H, He X Q (2018). A numerical simulation study on mechanical behaviour of coal with bedding planes under coupled static and dynamic load. Int J Min Sci Technol, 28(5): 791–797

Wu P F, Liang W G, Cao M T, Yang J F, Li L (2017). Experimental investigation on model I fracture characteristics of coal in different stratification orientation. Chin J Undergr Sp Eng.,13(Supp.2): 538–545 (in Chinese)

Yin H, Zhou J P, Jiang Y D, Xian X F, Liu Q L (2016). Physical and structural changes in shale associated with supercritical CO_2 exposure. Fuel, 184: 289–303

Zagorščak R, Thomas H R (2018). Effects of subcritical and supercritical CO_2 sorption on deformation and failure of high-rank coals. Int J Coal Geol, 199: 113–123

Zhang G L, Ranjith P G, Li Z S, Gao M Z, Ma Z Y (2021a). Long-term effects of CO_2-water-coal interactions on structural and mechanical changes of bituminous coal. J Petrol Sci Eng, 207: 109093

Zhang H, Hu Z C, Xu Y, Fu X X, Li W, Zhang D F (2021c). Impacts of long-term exposure to supercritical carbon dioxide on physicochemical properties and adsorption and desorption capabilities of moisture-equilibrated coals. Energy Fuels, 35(15): 12270–12287

Zhang Y B, Yao X L, Liang P, Wang K X, Sun L, Tian B Z, Liu X X, Wang S Y (2021b). Fracture evolution and localization effect of damage in rock based on wave velocity imaging technology. J Cent South U, 28(9): 2752–2769

Zhao P, He B, Zhang B, Liu J (2022). Porosity of gas shale: is the NMR-based measurement reliable? Petrol Sci, 19(2): 509–517

Zhao Y X, Gong S, Hao X J, Peng Y, Jiang Y D (2017). Effects of loading rate and bedding on the dynamic fracture toughness of coal: laboratory experiments. Eng Fract Mech, 178: 375–391